Strategies for mitigating the ionization-induced beam head erosion problem in an electron-beam-driven plasma wakefield accelerator

W An, M Zhou, N Vafaei-Najafabadi, K A Marsh, C E Clayton, C Joshi, W B Mori, W Lu, E Adli, Sébastien Corde, et al.

Strategies for mitigating the ionization-induced beam head erosion problem in an electron-beam-driven plasma wakefield accelerator

W. An,[1] M. Zhou,[1] N. Vafaei-Najafabadi,[1] K. A. Marsh,[1] C. E. Clayton,[1] C. Joshi,[1] W. B. Mori,[1,2] W. Lu,[3,2] E. Adli,[4,5] S. Corde,[5] M. Litos,[5] S. Li,[5] S. Gessner,[5] J. Frederico,[5] M. J. Hogan,[5] D. Walz,[5] J. England,[5] J. P. Delahaye,[5] and P. Muggli[6]

[1]*Department of Electrical Engineering, University of California Los Angeles, Los Angeles, California 90095, USA*
[2]*Department of Physics and Astronomy, University of California Los Angeles, Los Angeles, California 90095, USA*
[3]*Tsinghua University, Beijing, China*
[4]*Department of Physics, University of Oslo, 0316 Oslo, Norway*
[5]*SLAC National Accelerator Laboratory, Menlo Park, California 90309, USA*
[6]*Max Planck Institute for Physics, Munich, Germany*

(Received 11 June 2013; published 9 October 2013)

Strategies for mitigating ionization-induced beam head erosion in an electron-beam-driven plasma wakefield accelerator (PWFA) are explored when the plasma and the wake are both formed by the transverse electric field of the beam itself. Beam head erosion can occur in a preformed plasma because of a lack of focusing force from the wake at the rising edge (head) of the beam due to the finite inertia of the electrons. When the plasma is produced by field ionization from the space charge field of the beam, the head erosion is significantly exacerbated due to the gradual recession (in the beam frame) of the 100% ionization contour. Beam particles in front of the ionization front cannot be focused (guided) causing them to expand as in vacuum. When they expand, the location of the ionization front recedes such that even more beam particles are completely unguided. Eventually this process terminates the wake formation prematurely, i.e., well before the beam is depleted of its energy. Ionization-induced head erosion can be mitigated by controlling the beam parameters (emittance, charge, and energy) and/or the plasma conditions. In this paper we explore how the latter can be optimized so as to extend the beam propagation distance and thereby increase the energy gain. In particular we show that, by using a combination of the alkali atoms of the lowest practical ionization potential (Cs) for plasma formation and a precursor laser pulse to generate a narrow plasma filament in front of the beam, the head erosion rate can be dramatically reduced. Simulation results show that in the upcoming ''two-bunch PWFA experiments'' on the FACET facility at SLAC national accelerator laboratory the energy gain of the trailing beam can be up to 10 times larger for the given parameters when employing these techniques. Comparison of the effect of beam head erosion in preformed and ionization produced plasmas is also presented.

DOI: 10.1103/PhysRevSTAB.16.101301 PACS numbers: 52.40.Mj, 52.59.Bi, 52.59.Fn

I. INTRODUCTION

Earlier experiments at the Final Focus Test Beam facility at the Stanford Linear Accelerator Center (SLAC) [1] have shown that a plasma wakefield accelerator (PWFA) can sustain an accelerating gradient exceeding 50 GeV/m over almost a meter long distance. The large-amplitude plasma wave or wake was excited by a high energy electron beam operating in the so-called ''blowout'' regime [2,3], where the electron beam density n_b is much larger than the plasma density n_p or the beam current exceeds a few tens of kA. The plasma was formed in these experiments by ionizing a column of lithium (Li) using the transverse electric field E_r of the 42 GeV electron bunch [4]. When the high energy electron bunch (the drive beam) travels through the neutral gas, the E_r field of the beam ionizes the neutral gas into the plasma state. If $n_b > n_p$ (or if the beam current exceeds tens of kAs), it expels all the plasma electrons within a certain distance of the bunch thereby creating an ion cavity (resembling a bubble) around the beam. The expelled plasma electrons form a sheath around this ion cavity and are pulled back to the axis at the rear part of the bubble by the restoring force exerted by the plasma ions, thereby forming a classic wakefield configuration. This highly nonlinear plasma wake contains both a transverse focusing field (which increases linearly away from the axis with the transverse distance r) and a longitudinal accelerating field (which is uniform in the transverse direction), conditions that are ideal for accelerating an electron beam. The amplitude of the longitudinal electric field in such a nonlinear plasma wake can be on the order of $m_e c\omega_p/e \approx 10\ [\mathrm{GV/m}]\sqrt{n_p/10^{16}\ [\mathrm{cm}^{-3}]}$, where n_p is the plasma density and ω_p is the plasma frequency [5]. While the drive beam transfers its energy to the wake, a second electron bunch (the trailing beam) placed at an

appropriate distance behind the drive beam, i.e., in the accelerating field of the wake, gains energy. If the trailing beam contains a sufficient number of electrons it can load the wake and flatten the accelerating field [6] so that all the electrons gain energy at nearly the same rate, thus minimizing the energy spread of the beam and increasing the energy extraction efficiency. Such a "two-bunch" PWFA scenario will be tested on the newly completed facility FACET at SLAC [7].

In the drive beam-trailing beam scenario described above, it is imperative that the drive beam transfer most of its energy to the plasma wake in order to efficiently transfer energy to the trailing beam. Since both the drive and the trailing beams are usually highly relativistic there is no significant relative motion between the two until the drive beam has lost most of its energy. This allows high efficiency in principle. However, because of the excessive beam head erosion, the acceleration distance and hence energy gain can be terminated if the drive beam is no longer able to create the plasma (and therefore the wake) through the field ionization process. In this case the energy gain of the particles in the trailing bunch is not limited by the energy depletion of the drive beam (pump depletion) but by head erosion. When the plasma is produced by E_r of the drive beam that has a temporally rising charge distribution, then the front of the beam (before the ionization threshold has been reached) expands as if it were in vacuum. Once the ionization threshold is exceeded, then the beam begins to ionize the gas and expel the plasma electrons. However, due to the finite inertia of the electrons, the ion channel is not formed immediately after the ionization front and the focusing force of the ions is thus not strong enough to confine electrons behind the ionization front until enough plasma electrons have been blown out. This leads to different longitudinal slices of the beam expanding

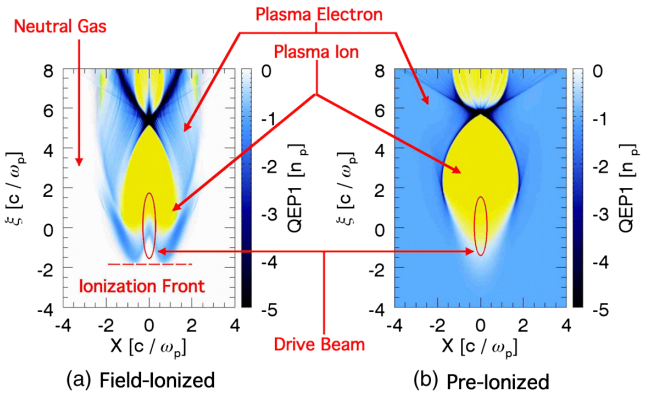

FIG. 1. Snapshot of the plasma electron density from the wake exited by an electron beam in (a) a field-ionized lithium plasma (the plasma ions are shown in yellow and the area in white is filled by the neutral atoms that are not ionized) and (b) a preformed plasma. The plots are a 2D cross section at the center of the 3D simulation box. The drive beam (shown as the red contour) is moving downwards.

laterally at different rates because of their finite emittance, albeit at a rate smaller than they would if they were propagating in vacuum. This reduces the E_r from the beam near the ionization front causing it to recede backward in the beam frame and leading to an even smaller portion of the beam to be confined. As more of the beam is not confined and the ionization front recedes, a portion of the wake becomes smaller until eventually the wake can no longer be excited.

Figure 1 illustrates the phenomenon of beam head erosion by comparing the propagation of otherwise identical drive beams through either a neutral lithium gas (where it produces plasma via field ionization) or through a preformed plasma with a transverse radius much larger than the electron blowout radius R_b caused by the drive beam. The preformed plasma density and the neutral Li gas density are both 5×10^{16} cm^{-3}. The drive beam contains $N = 9.6 \times 10^9$ electrons. It has a Gaussian profile and the rms spot size of the beam is $\sigma_r = 10$ μm $(0.42c/\omega_p)$. The rms pulse length of the beam is $\sigma_z = 34.1$ μm $(1.43c/\omega_p)$. The initial energy of the beam is 22.5 GeV. The 3D parallel quasistatic particle-in-cell code QUICKPIC [8,9] is used for the simulations. The simulation box uses the coordinate $\xi = ct - z$ instead of z in the longitudinal direction, which is equivalent to following the beam in the speed of light frame. The initial drive beam center is at $\xi = 0$, and the beam is moving downwards in the simulation box.

In contrast to the case of the fully preformed plasma which is initially uniform [see Fig. 1(b)], the field-ionized plasma shown in Fig. 1(a) has a "W" shape contour at the beam head because the beam's Coulomb field is not strong enough to ionize the neutral gas near the axis of the beam, i.e., recall that for a cylindrically symmetric, transversely Gaussian beam the E_r is zero on axis. Nevertheless in both cases a region of complete electron blowout does exist and the position where the expelled plasma electrons return to and cross the axis (also the position where the accelerating field is at its maximum) is at almost the same location, whereas in the preformed plasma case the expelled electrons form a very thin sheath around the ions, and in the self-ionized case this sheath is somewhat diffused. As time progresses, and as the beam propagates further into the gas, the ionization front recedes further and further (in the beam frame) and eventually limits the distance over which the beam can form the wake as discussed earlier.

The rate at which the ionization front recedes, i.e., the "etching speed," can be used as a figure of merit to quantify the beam head erosion. The slower the etching speed, the longer is the distance over which a plasma wake can be sustained. In Ref. [10], the etching speed was found to be a constant for a drive beam with a flattop longitudinal profile, being proportional to $\epsilon_N/\gamma N^{1.5}$, where ϵ_N is the normalized emittance of the beam, γ is the beam Lorentz factor, and N is the beam particle number. Thus we can

mitigate the head erosion by reducing the emittance ϵ_N or increasing the beam particle number (N) or energy of the beam γ. For fixed beam parameters the only other way to mitigate the beam head erosion is to manipulate the plasma source. In this paper we explore two techniques for doing this. The first is to use a neutral gas with as low an ionization potential as possible so that the onset of ionization will occur sooner during the rise time of the beam. The second is to use a precursor laser pulse to form a very narrow plasma filament. We have found that both techniques (particularly when used together) dramatically reduce the beam etching speed and thereby increase the distance over which the beam can form the wake. These two aspects will be discussed in Secs. II and III. In Sec. IV, we compare the simulation results of the possible two-bunch PWFA experiments for FACET with and without these techniques. In the last Sec. V, we summarize the results.

II. DEPENDENCE OF THE ETCHING SPEED ON THE IONIZATION POTENTIAL

Different neutral atoms have different electron ionization potentials. For PWFA experiments a long column of neutral gas that typically has a low ionization potential is used. Using the Ammosov-Delone-Krainov model [11], we can calculate each gas's ionization threshold E_{th}, defined as the external DC electric field at which the neutral gas can be fully ionized during a given time duration. This model has been shown to give reasonable agreement in experiments where the peak electric field of a 23.5 GeV electron beam necessary for the ionization of different simple and complex gases (noble, diatomic homopolar, polyatomic, and monoatomic metal vapor) was determined [12]. In this work we consider different group 1 alkali metal atoms because they have a very low threshold E_{th} for the outermost electron to be ionized and a relatively larger difference between the ionization potentials of the first and the second electron (see Fig. 2).

Figure 2 shows the fractional ionization of different group 1 alkali metal atoms as the magnitude of E field is increased. The ionization time duration is chosen to be 50 fs (which is the rise time of a typical electron beam pulse length in PWFA experiments). From this plot, we can see that for fully ionizing ($> 99\%$) the first electron [Fig. 2(a)] the threshold electric field E_{th} is 6.4 GV/m for Li, 4.3 GV/m for K, 4.0 GV/m for Rb, and 3.5 GV/m for Cs, and for fully ionizing ($> 99\%$) the second electron E_{th} is 409.2 GV/m for Li, 90.8 GV/m for K, 69.5 GV/m for Rb, and 51.8 GV/m for Cs. This large gap of E_{th} between the first and the second ionization is one reason why it is possible to generate 100%, singly ionized metal-vapor plasmas using the self-field of a short, dense electron beam. Nevertheless under certain conditions, the combined accelerating field of the wake E_z and the E_r of the beam can cause ionization of the second electron which can inject dark current into the plasma accelerator structure [13]. One therefore has to choose the right beam and plasma parameters so that $\sqrt{E_r^2 + E_z^2}$ should be smaller than E_{th} for the second electron.

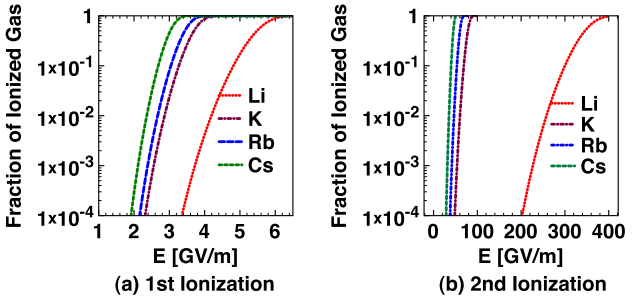

FIG. 2. Fraction of ionized gas vs electric field (assumed to be constant for 50 fs).

The first generation of PWFA experiments used Li vapor to generate field-ionized plasmas. However, the ionization potential of the heavier alkali metal atoms becomes progressively smaller (5.4 eV for Li vs 3.9 eV for Cs for the outermost electron) with a corresponding decrease in the electric field needed to fully ionize them as stated earlier. This in turn means that as the drive beam propagates through a column of say Cs vapor compared to Li vapor, ionization will occur sooner during the rise time of the pulse and the rate at which the ionization front recedes as the beam propagates further into the vapor will be smaller.

To quantify this ionization potential dependence on the head erosion speed, we have carried out several QUICKPIC simulations with the same electron beam parameters but with the beam propagating through different alkali vapor columns. The electron beam has a flattop longitudinal profile and a Gaussian transverse profile. The beam contains $N = 9.6 \times 10^9$ electrons, its rms spot size is $\sigma_r = 10\ \mu$m ($0.42c/\omega_p$), and its pulse length is $L = 85.5\ \mu$m ($3.59c/\omega_p$). The normalized emittance of the beam is $\epsilon_N = 150$ mm mrad and the initial energy of the beam is 22.5 GeV (the energy of the beam particle is fixed during the simulation in order to eliminate the dependence of the etching speed on the beam energy). The initial neutral gas density is 5×10^{16} cm^{-3}. Figure 3 shows the beam evolution in neutral Li.

We can see from Fig. 3 that the ionization front moves backwards in the frame of the beam during its propagation due to continuous expansion of the front slices of the beam. After around 50 cm of propagation, the remainder of the beam is no longer able to form the wake and, as a consequence, an on-axis hole in the plasma (due to the on-axis E_r being below the ionization threshold) is evident. We can visualize the recession of the ionization front by plotting the on-axis amplitude of the accelerating electric field E_z of the plasma wakefield at different propagation distances, $E_z(r = 0, \xi, s)$ as shown in Fig. 4 for the alkali metals Li, K, Rb, and Cs.

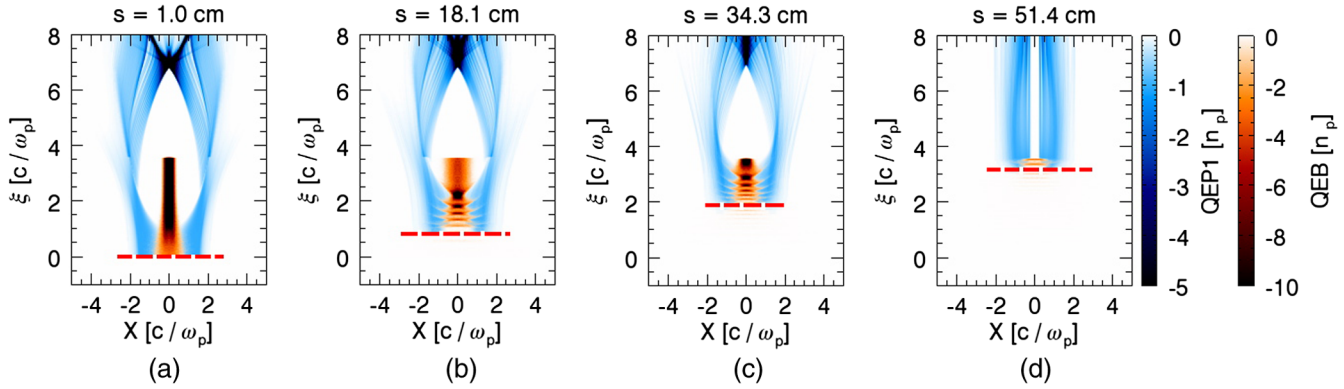

FIG. 3. Beam head erosion in the field-ionized lithium plasma. The plasma electron density has the blue color and the beam density is in brown. $\xi = ct - z$ is the distance in the speed of light frame and $s = z$ is the propagation distance in the lab frame. Dotted lines in (a)–(d) show the position of the ionization front.

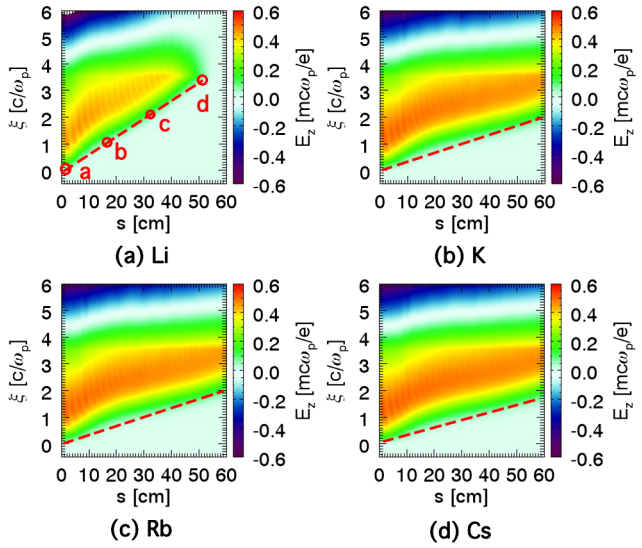

FIG. 4. E_z evolution during the beam propagating in different alkaline metal gases. The beam is moving downwards. The four circles in (a) correspond to the positions of the ionization fronts shown in Fig. 3.

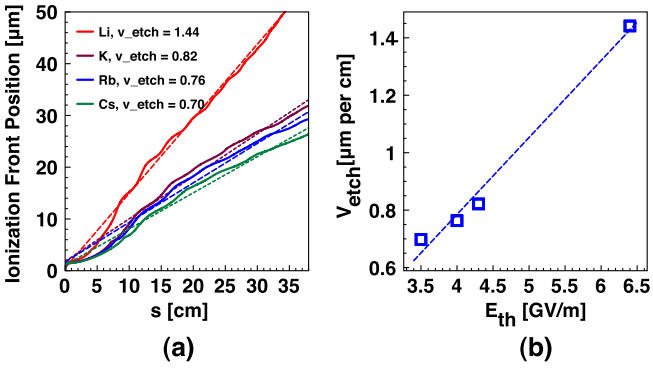

FIG. 5. Ionization front etching in different gases: (a) receding of the ionization front in different alkaline metal gases; (b) the etching velocity verses the neutral gas ionization threshold.

In these plots, the red dashed line shows the trajectory of the onset of the wakefield (a contour for $E_z = 0.1$). The line has a positive slope indicating that the ionization front is receding as the beam propagates in the plasma. In the Li gas, the plasma wake is gone at around $s = 50$ cm, which is the same distance as that shown in the Fig. 3. But in other neutral gases with lower ionization potential than Li, the slopes are progressively smaller indicating that the plasma wakes can be sustained over a longer distance. We define the etching speed for the different gases to be the slope of the dashed red lines. In Fig. 5 we plot the etching speed for the various gasses.

Figure 5(b) shows that the etching velocity is linearly proportional to the ionization threshold [10] indicating that as expected it is better to use a neutral gas with as low an ionization threshold as possible like Rb or Cs to slow down speed at which head erosion occurs if field ionization is employed to both produce the plasma and excite the wake.

III. FURTHER MITIGATION OF THE HEAD EROSION RATE USING A LASER-PRODUCED PLASMA FILAMENT

As already shown by the comparison of the snapshot of Fig. 1(a) with that of Fig. 1(b), in a preformed plasma the phenomenon of beam head erosion is relatively unimportant, as one would expect. Using the E_z time-evolution format of Fig. 4, the effects of additional preformation of a plasma in Li is shown in Fig. 6 for various preplasma conditions. These range from the extremes of the fully preformed plasma of Fig. 6(a) to that of field ionization only with no preformed plasma as in Fig. 6(c), together with the interesting intermediate case of Fig. 6(b), where the plasma is preformed over a much smaller volume, i.e., only along a narrow filament. The electron beam used in the simulation has the same parameters as those in the last section except it now has a Gaussian (rather than flattop) longitudinal profile with a pulse length $\sigma_z = 34.1\ \mu$m $(1.43c/\omega_p)$.

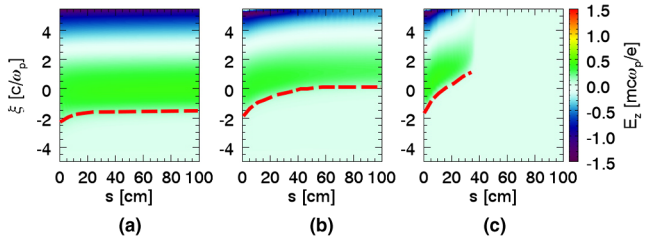

FIG. 6. E_z evolution during the beam propagating in (a) a fully preformed plasma; (b) a field-ionized Li plasma with the narrow plasma filament; (c) a field-ionized Li plasma. The Gaussian beam suffers little head erosion in a preformed plasma but rapidly erodes in the field-ionized plasma.

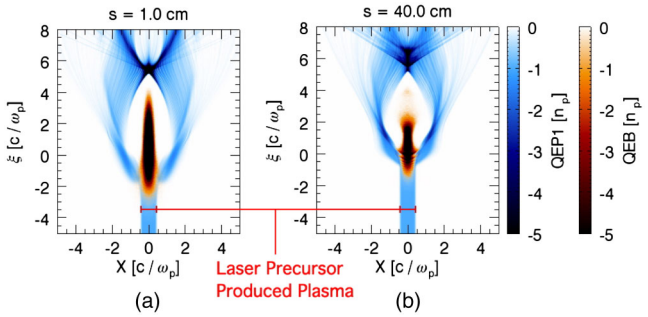

FIG. 7. Density snapshots of the plasma wake with a small preformed Li plasma column. The plasma electron density has the blue color and the beam density is in brown.

One can immediately see from Fig. 6(a) that in contrast to the self-ionized plasma case depicted in Fig. 6(c) there is almost no head erosion in the preformed Li plasma. (Note that the slope of the red dashed line in this figure is not constant because the beam now has a Gaussian current profile.)

Unfortunately, it is not easy to produce large diameter, uniform density plasmas in the $1.0\times10^{16}\sim5.0\times10^{17}\,\mathrm{cm}^{-3}$ range. To fully ionize the gas in front of the drive beam, a laser pulse that tunnel or multiphoton ionizes the gas ahead of the drive beam can be used. The drive beam can then excite the plasma wake in this preformed plasma. The radius of the preformed plasma column should be larger than several times the blowout radius of the wake. This in turn implies that the laser pulse should have enough energy to maintain the intensity above the ionization threshold over the entire volume of the gas that needs to be converted into plasma. This can require rather expensive laser infrastructure particularly if plasma columns that are several meters in length are needed.

We therefore explored whether a laser precursor pulse that generates only a narrow filament of Li plasma in front of the drive beam is sufficient to drastically reduce the beam head erosion. In this case the laser beam ionizes a plasma column that is only σ_r (the beam spot size) in radius. The Li plasma is then preproduced by the laser pulse whose radius is the same as the beam radius and much smaller than the blowout radius R_b. This allows the very front of the beam, where the beam's E_r is too weak to ionize the neutral Li gas, to be guided, thereby greatly reducing the rate of ionization-induced head erosion. Such narrow but long plasma columns can be produced using axicon (a conically formed refractor element forming an extended line focus) optics to focus the laser pulse. Figure 7 shows density plots from a simulation depicting the propagation of the drive beam in a narrow preformed plasma column.

In this simulation, we use lithium for the gas and the preformed plasma column has a radius of 10 μm, which is equal to the spot size of the electron beam. Although the plasma filament is not wide enough to include the whole bubble of the wake, it can provide a fully ionized plasma region for the head of the beam. The Coulomb field of the main part of the electron beam subsequently ionizes the neutral gas around the narrow plasma filament allowing a wake to be formed. The two plots correspond to when the electron beam enters the plasma [Fig. 7(a)] and after it has propagated 40 cm into the plasma [Fig. 7(b)].

Returning now to Fig. 6 we compare the result [in Fig. 6(b)] of axial Li preionization with that of full volume Li preionization [Fig. 6(a)], where we see that the performance in terms of beam persistence is nearly as good, with excellent propagation beyond 100 cm. This is because the head of the beam can now expel plasma electrons in the filament thereby providing a focusing force on the front slices of the electron beam as in the preformed case keeping it from expanding and thus reducing the head erosion rate. In comparison, the result with no Li preionization [Fig. 6(c)] is disastrous (rapid erosion and ionization front movement resulting in a much shorter penetration of about 30 cm). The method of axial Li preionization can drastically reduce the energy required in the laser pulse by a factor of $(R_b/\sigma_r)^2$, thereby making the laser infrastructure needed more manageable. We have also used cesium for the gas. For these beam parameters the head erosion looks similar while the wake looks better for cesium because the gas is ionized out to a radius closer to the blowout radius.

IV. TWO-BUNCH PWFA SIMULATIONS

We next investigate the use of a laser precursor and the choice of either lithium or cesium for the oven gas with parameters of relevance to the upcoming two-bunch experiments at FACET. As discussed earlier, by employing lower ionization energy atoms and/or a laser precursor to form a thin plasma filament ahead of the drive beam it is possible to mitigate the head erosion rate. We now show that it is possible to propagate the drive beam until it is efficiently depleted of its energy while forming a high gradient wake by combining both the precursor and cesium gas for the FACET parameters. We also show that by beam loading such a wake with a trailing beam it is possible to transfer much of the energy in the wake to this trailing

beam while obtaining a narrow energy spread. We simulated such a two-bunch PWFA scenario in the field-ionized Li plasma and then, in view of the behavior seen in Li, again in a Cs plasma, with results for both shown in Figs. 8 and 9. In Fig. 8(a) we show the plasma and beam densities for the Li case as the beams enter the gas.

In the simulation, the drive beam parameters are the same as the ones used in the last section. However now a trailing beam which contains $N = 4.3 \times 10^9$ electrons is also included. The rms spot size of this beam is $\sigma_r = 10\ \mu\text{m}\ (0.42c/\omega_p)$. The rms pulse length of the beam is $\sigma_z = 19.3\ \mu\text{m}\ (0.81c/\omega_p)$. The normalized emittance of the beam is $\epsilon_N = 150$ mm mrad and the energy of the beam is 22.5 GeV. Both the drive beam and the trailing beam have a Gaussian density profile, and the distance between two beams' centers is 130 μm $(5.46c/\omega_p)$. The plasma density is $5 \times 10^{16}\ \text{cm}^{-3}$, which is properly chosen so that the plasma wake contains the trailing beam in the accelerating phase of the wake.

The beams' energy spectra after propagation through the Li plasma are shown in Fig. 9(a). As a comparison, we also show the beams' spectra after 200 cm acceleration in a fully preformed Li plasma in the same plot. We explored the use of different gas densities. The tradeoff is that for higher densities the blowout radius is less so a narrow ionization column is needed (allowing lithium to be used) while on the other hand at high densities the wake wavelength is shorter and the spacing between the drive and trailing beams will be too short. The plasma density used represents a starting choice for the FACET parameters where the beam parameters including the spacing and charge are fixed. Note that the drive beam parameters are identical to the case shown in Fig. 7(a) but that the beam appears longer in Fig. 7(a) because the beam has been pinched.

We can see that in the fully preformed plasma [brown curve in Fig. 9(a)] the trailing beam obtains an energy gain of around 30 GeV (at an average rate of 15 GeV/m) while more importantly the full width at half maximum (FWHM) energy spread is around 5% (note that this energy spread

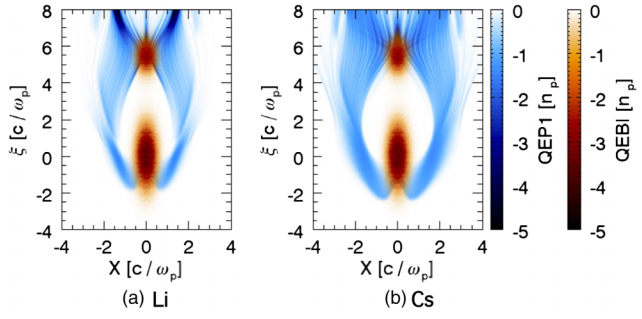

FIG. 8. Snapshot of a two-bunch PWFA in (a) a field-ionized Li plasma (b) a field-ionized Cs plasma. The plasma electron density has the blue color and the beam density is in brown.

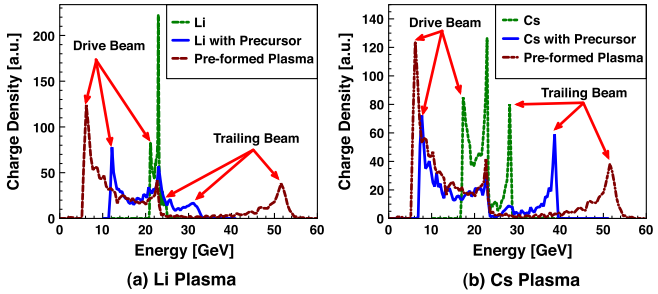

FIG. 9. Energy spectra of the drive beam and the trailing beam at the end of the acceleration: (a) in a field-ionized Li plasma; (b) in a field-ionized Cs plasma.

can be reduced further by optimizing the preformed plasma density for a given drive-trailing beam combination). The energy transfer efficiency from the drive to the trailing beam is 69.3%.

However, if we use the beam's self-field to ionize the Li vapor the acceleration length is only 16.7 cm and the energy gain of the trailing beam is only 2 GeV [the green line in Fig. 9(a)]. The large spike in the middle of the spectrum shows that a considerable fraction of the electrons in the drive beam does not lose energy due to head erosion. The maximum energy loss of the drive beam electrons is around 2 GeV.

If however the head erosion is mitigated by using a plasma filament that has a radius of 10 μm, which is equal to the drive beam spot size then there is some additional energy gain as the drive beam now propagates further. The blue line in Fig. 9(a) shows the energy spectrum of two beams at $s = 171.3$ cm where the acceleration terminates. The energy gain of the trailing beam increases to around 10 GeV due to the reduced the beam head erosion rate. This is a factor of 5 improvement in energy gain compared with the case of no preplasma, but still only one-third of the energy gain with full preplasma.

Although the energy gain on the trailing beam has indeed been increased over the case with no preplasma by employing the plasma filament in Li, the energy spread is no better and is much worse than when a fully preformed plasma is used. This is because the drive beam is simply not intense enough to ionize the plasma to the distance of one R_b [as shown in Fig. 8(a)], which is necessary to form a nice ion cavity as it does in the completely preionized case discussed above. However, if one now uses Rb or Cs instead of the Li, the same drive beam can ionize a plasma column out to a larger radius for the same beam parameters and form a wake that resembles the wake formed in a completely preionized plasma. Figure 8(b) shows the density plot of the same two-bunch PWFA case but in a field-ionized Cs plasma. Compared with Fig. 8(a), the plasma wake shows an ion cavity clearly enclosed by the electron sheath in Cs than that in Li. Most of the trailing bunch is now inside the bubble.

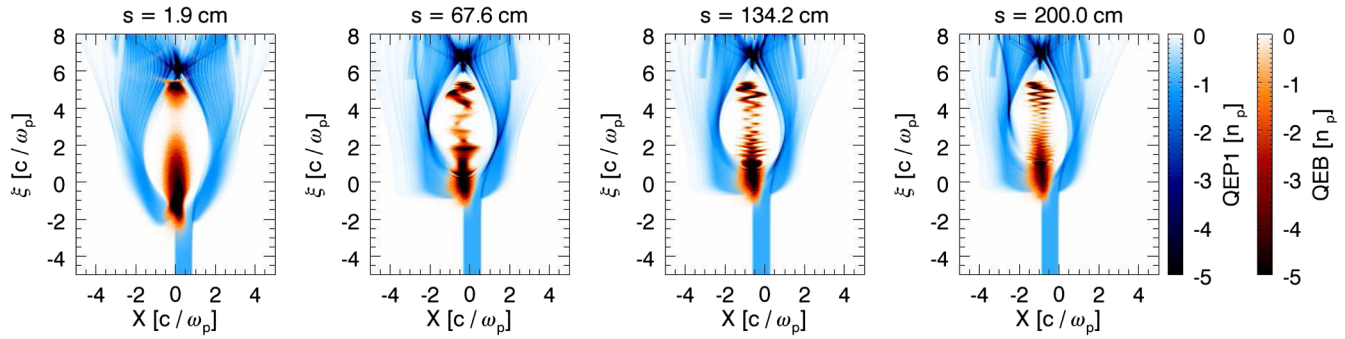

FIG. 10. Snapshots of beam and plasma densities from the simulation where the laser precursor drifts to the left in the rest frame of the beam.

Figure 9(b) shows the energy spectra of the same beams using field-ionized Cs plasma (the green line). Now, the acceleration length has increased to 76.2 cm, which is longer than the 16.7 cm observed in Li. The energy gain of the trailing beam is consequently increased to 5 GeV (from 2 GeV value for Li) and the energy spread is narrower. Now when one uses a 10 μm radius plasma filament in front of the Cs plasma the acceleration length reaches 200 cm. From the energy spectrum [the blue line in Fig. 9(b)], one can see that the energy gain of the trailing beam is around 20 GeV and the FWHM energy spread of the trailing beam is around 3%.

When using the laser precursor to ionize the plasma filament in front of the beam, the alignment accuracy between the laser precursor and the drive beam will affect the acceleration. We have explored the effect of an alignment error via a simulation that has a 10 μrad angle between the propagation directions of the laser precursor and the drive beam. At the entrance of the plasma, the center of the laser precursor pulse is offset by 10 μm (which is equal to the electron beam spot size) from the center of the drive beam. Since the laser precursor propagates with an angle to the drive beam, the plasma filament ionized by the laser will drift at a small speed (which is 10 μm every meter the laser propagates when the angle is equal to 10 μrad) along the transverse direction in the rest frame of the beam. The density snapshots from the simulation are shown in the Fig. 10.

Although there is a misalignment between the laser precursor and the drive electron beam, the acceleration still lasts for 200 cm. The final energy gain on the trailing beam is almost the same as that with the aligned laser precursor. But as the laser pulse and therefore the plasma filament drift to the left in the simulation box, the drive beam as well as the trailing beam also drift to the left together with the plasma filament. This appears to strongly seed the hosing instability on the beams, especially on the trailing beam. In the experiments, the hosing motion of the trailing beam will cause particle loss as the beam propagates between the plasma exit and the spectrometer. The hosing motion of the beam will also generate more betatron radiation. In fact alignment accuracy of the laser pulse and the electron beams can be optimized in the experiments by monitoring the betatron x-ray radiation coming out of the plasma. When the laser and the drive beam are aligned, the radiation will reach its smallest value.

It should also be pointed out that when we use a neutral gas with lower ionization threshold such as Cs or Rb, the second ionization threshold becomes smaller as well. In Sec. II, we have showed that the second ionization threshold for Cs is 51.8 GV/m, which is close to the electric field magnitude of the plasma wake. Therefore, it is possible that the second ionization of Cs occurs under some situations. If this happens inside the plasma bubble, the plasma wakefield may trap the ionized electrons and accelerate them into a high energy. But the number of the electrons produced from the second ionization is much less than that of the trailing beam. So the acceleration of the trailing beam should not be affected in this case. In other cases with more dense and shorter drive beams propagating in a higher density plasma, this additional ionization of the second electron inside the wake can act as a source of dark current that depletes the energy from the wake [13].

V. SUMMARY

In this paper, we have devised strategies for mitigating the drive beam head erosion in a PWFA that employs the beam's self-field to produce the plasma. The head erosion affects the drive beam's ability to ionize the neutral gas and therefore form the wake and thus terminates the acceleration process even though the drive beam still contains much energy. Although this problem is not significant in a fully preformed plasma it has proved difficult to generate large volume, high density, uniform plasmas needed for PWFA. However, we find that head erosion in a field-ionized plasma can be mitigated by employing a combination of lower ionization threshold gas and a laser-produced plasma filament in front of the drive beam. These strategies will be employed in the upcoming two-bunch PWFA experiments on the FACET facility. Finally, we repeat that the beam head erosion problem may also be mitigated by a combination of reducing the beam emittance, increasing the beam current and energy.

ACKNOWLEDGMENTS

This work was supported by the U.S. Department of Energy under Grants No. DE-SC0008491, No. DE-FG02-92-ER40727, No. DE-SC0008316, and No. DE-SC0007970, and by the National Science Foundation under Grants No. PHY-0936266, No. PHY-0960344, and No. PHY-0934856. The simulations were carried out on the UCLA Hoffman 2 and Dawson 2 Clusters, and the resources of the National Energy Research Scientific Computing Center, the National Center for Supercomputing Applications and National Center for Computational Sciences.

[1] I. Blumenfeld *et al.*, Nature (London) **445**, 741 (2007).
[2] J. B. Rosenzweig, B. Breizman, T. Katsouleas, and J. J. Su, Phys. Rev. A **44**, R6189 (1991).
[3] W. Lu, C. Huang, M. Zhou, W. B. Mori, and T. Katsouleas, Phys. Rev. Lett. **96**, 165002 (2006).
[4] P. Muggli, K. A. Marsh, S. Wang, C. E. Clayton, S. Lee, T. C. Katsouleas, and C. Joshi, IEEE Trans. Plasma Sci. **27**, 791 (1999).
[5] C. Joshi *et al.*, Phys. Plasmas **9**, 1845 (2002).
[6] M. Tzoufras, W. Lu, F. Tsung, C. Huang, W. Mori, T. Katsouleas, J. Vieira, R. Fonseca, and L. Silva, Phys. Rev. Lett. **101**, 145002 (2008).
[7] M. J. Hogan *et al.*, New J. Phys. **12**, 055030 (2010).
[8] C. Huang, V. K. Decyk, C. Ren, M. Zhou, W. Lu, W. B. Mori, J. H. Cooley, T. M. Antonsen, and T. Katsouleas, J. Comput. Phys. **217**, 658 (2006).
[9] W. An, V. K. Decyk, W. B. Mori, and T. M. Antonsen, J. Comput. Phys. **250**, 165 (2013).
[10] M. Zhou, Ph.D. thesis, University of California Los Angeles, 2008.
[11] D. L. Bruhwiler, D. A. Dimitrov, J. R. Cary, E. Esarey, W. Leemans, and R. E. Giacone, Phys. Plasmas **10**, 2022 (2003).
[12] C. O'Connell *et al.*, Phys. Rev. ST Accel. Beams **9**, 101301 (2006).
[13] N. Vafaei-Najafabadi *et al.* (to be published).